Validating a Device for Whiplash Motion Simulation in a Porcine Model

Validating a Device for Whiplash Motion Simulation in a Porcine Model

N. Soltan[1], P.A. Cripton[1,2], M.Y. Svensson[3], G.P. Siegmund[4,5]
[1]Department of Mechanical Engineering, University of British Columbia; [2]School of Biomedical Engineering, University of British Columbia, [3]Department of Mechanics and Maritime Sciences, Chalmers University of Technology, [4]MEA Forensic Engineers & Scientists, [5]School of Kinesiology, University of British Columbia

ABSTRACT

Whiplash injury is a common outcome following minor automobile collisions. One theorized mechanism for whiplash injury is that the rapid head and neck motions induced by a collision can injure nerve cells in the dorsal root ganglia through pressure gradients developed in the spinal canal and surrounding tissues. This injury mechanism has previously been studied in human cadaver and porcine models. However, the whiplash motion simulation methods in the latter studies lacked the control necessary to explore the independent effects of head rotation and retraction on the measured spinal pressures. This project aimed to address the limitations of previous porcine whiplash studies by developing and validating a new whiplash motion simulation device to enable further study of this injury mechanism. The new proposed device consists of two servomotors which can be programmed to precisely actuate a headplate through mechanical linkages. For the current study, an inert surrogate model was used for preliminary testing of the device using a whiplash motion profile from previous porcine studies. The time scale of the motion profile was adjusted to incrementally increase severity. The positional accuracy and repeatability of the device was assessed through marker tracking of the headplate and logging of the motor encoder positions. Angular rates and linear accelerations of the plate were also measured. Testing demonstrated the strengths of the proposed device in accurately and repeatably replicating programmed motion profiles. Some design modifications can potentially enable simulating whiplash motion severities commensurate with previous porcine whiplash studies. With future testing using this device, our understanding of the pressure-induced whiplash injury mechanism can be improved, which can inform effective treatments and preventative measures for whiplash injury.

INTRODUCTION

Despite their prevalence and large economic/social burden, neck sprains and strains, commonly referred to as whiplash injuries, remain one of the most poorly understood automotive injuries (Siegmund et al., 2009). Associated symptoms of whiplash include neck and upper body pain, headache, dizziness and other cognitive/psychological symptoms (Croft et al., 2002;

Siegmund et al., 2009). Chronic disabling symptoms from whiplash injury account for a significant portion of overall disability from motor vehicle injuries (Sterner et al., 2004). In the United States alone, the cost of these injuries is estimated to exceed $19 billion annually (Croft et al., 2002).

A current challenge with effectively treating and preventing whiplash symptoms is the absence of observable tissue damage in patients and the lack of consensus on the mechanism of injury (Curatolo et al., 2011). Several anatomical sites and injury models have been hypothesized to be the source of whiplash injury. One such injury model proposes that the rapid extension-flexion of the neck during a collision ("whiplash motions") causes pressure gradients to develop in the spinal canal and across the vein bridges in the intervertebral foramina. These pressure gradients are theorized to increase tissue stress and cause nerve cell damage in the dorsal root ganglia (DRG) (Aldman, 1986; Svensson et al., 1993; Örtengren et al., 1996; Svensson et al., 2000).

During a rear-end collision, occupants in the impacted vehicle initially experience a retraction of the head relative to the torso as the head is not in contact with the head restraint. This retraction causes the upper and lower cervical spine to enter flexion and extension, respectively. Once the natural range of retraction is reached, the neck may transition into a fully extended posture and subsequently upon interacting with the head rest, enter a flexed posture (Ono et al., 1993; Svensson et al., 2000). It has been demonstrated that the volume of the spinal canal reduces and increases in extension and flexion, respectively (Yao et al., 2016). Therefore, it is theorized that the above-described whiplash motions and localized volume changes can cause the incompressible blood and cerebrospinal fluid in the spinal canal to displace and consequently form transient pressure gradients along the spinal canal and across the intervertebral foramina. This pressure effect is postulated to stress and strain the DRG, which are structures in the dorsal nerve roots and which are located in the intervertebral foramen. The DRG house the cell bodies of afferent nerves, therefore, direct injury to this site can explain many of the common whiplash symptoms (Siegmund et al., 2009).

This pressure-induced whiplash injury mechanism has previously been studied in porcine and human cadaver models. Through exposing anaesthetized pigs to simulated whiplash motions, Svensson et al. (1993) observed pressure pulses in the cervical spinal canal. The initial large pressure pulses appeared to correspond to the point of maximum neck retraction indicating the potential relevance of this phase of whiplash motion in producing injury. Following whiplash exposure, histopathological examination of the cervical DRG indicated plasma membrane leakage in the nerve cells of the exposed animals demonstrating cell dysfunction (Örtengren et al., 1996). This pressure effect was similarly demonstrated in post-mortem human subjects exposed to rear-end collisions, though tissue damage was not observable as in the *in vivo* experiments (Eichberger et al., 2000).

Despite establishing the foundational knowledge behind this whiplash injury mechanism, questions remain about the relative contributions of several head and neck kinematic parameters during whiplash motions to the pressure pulse magnitudes and whiplash injury risk. In the previous porcine whiplash studies (Svensson et al., 1993), the method of generating whiplash motions could not be used to study the independent effect of neck retraction distance and extension angle on the measured spinal pressure magnitudes. Understanding the influence of these kinematics parameters

on the pressure pulse magnitudes and whiplash injury risk can inform the design of motor vehicle safety systems for effective prevention of this injury. Thus, the objective of this project is to test and validate a custom-built device that aims to simulate whiplash motions with precise movement control. Specifically, we aim to 1) assess whether the proposed device is able to replicate the motion profiles tested in previous porcine whiplash studies, and 2) characterize the accuracy and repeatability of the simulated whiplash motions. This assessment will inform any device design modifications in order to enable further study of the DRG whiplash injury mechanism in an *in vivo* porcine model.

METHODS

Porcine Model

The whiplash device was designed to allow for further study of whiplash in an *in vivo* porcine model for several reasons. Firstly, our aim is to ultimately study the effect of whiplash motions on the dynamics and responses of a living system. Live tissue is needed to produce the proposed whiplash injury mechanism (cellular damage in the DRG). Additionally, it is unclear how the absence of arterial blood pressure in a cadaveric model affects the spinal pressure measurements (Eichberger et al., 2000).

Furthermore, the vertebral column of the pig in particular has gross similarities to the human vertebral column in terms of size and anatomy (Busscher et al., 2010; Sheng et al., 2010, 2016) and serves as a reasonable qualitative surrogate. The porcine model has been used in prior biomechanical studies in the context of whiplash (Svensson et al., 1993), spinal cord (Jones et al., 2012; Lee et al., 2013), and traumatic brain injury (Duhaime, 2006).

Device design

The custom whiplash device was designed and built at MEA Forensic Engineers & Scientists (Figure 1). The device consists of a frame which holds two rotary servomotors (Yaskawa, SGMCS-2ZN, Japan) with a rated torque and speed of 200 N·m and 150 rpm, respectively. The motors can achieve an instantaneous maximum torque of 600 N·m at zero speed. Each servomotor is equipped with a 20-bit encoder which allows for position feedback control. A series of mechanical linkages are attached to the motors on one end and a biteplate on the other end via ball joints. Using this device, the anaesthetized animal will be placed on the operating table with its head cantilevered off of the table edge and the biteplate will be secured in the animal's mouth. The combined rotation of the motors will be used to translate and rotate the biteplate to control and simulate programmed whiplash motions.

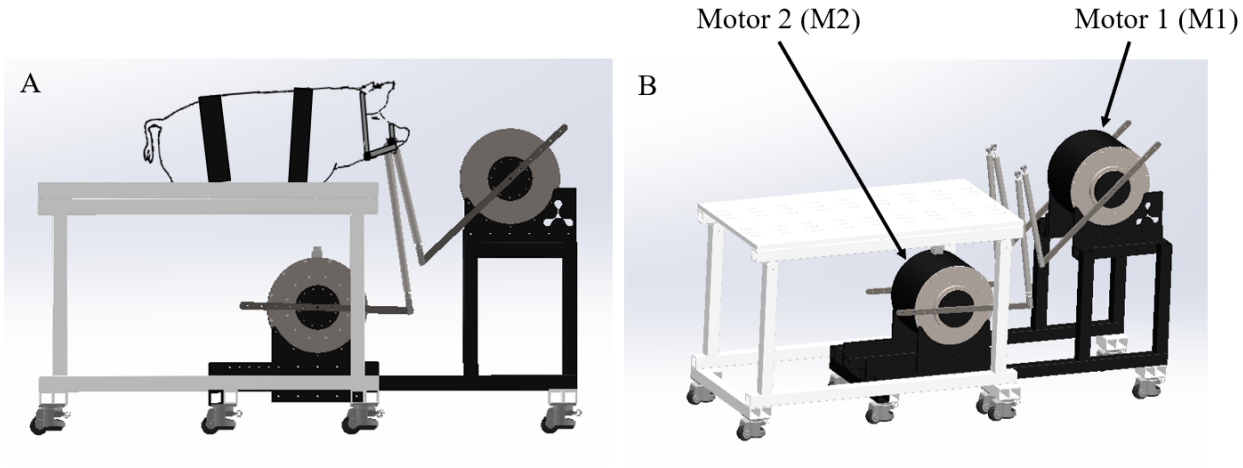

Figure 1: Whiplash apparatus. A: Side view, B: Isometric view (biteplate not shown).

This device design aims to address some of the limitations of the apparatus used in the previous porcine whiplash studies (Svensson et al., 1993). Our device and the previous apparatus primarily differ by the method used to generate the whiplash motions. With the previous device, whiplash motions were generated using a pre-tensed rubber-strap which transmitted force to a headplate. The animal was placed laterally on an operating table with its heads affixed to the headplate which was freely movable in the horizontal plane. Depending on the tension of the strap, the pull-force on the headplate could be adjusted with an accuracy of ± 20-100 N (Svensson et al., 1993). This design allowed for free motion of the animal's head and maximum neck extension angles were determined by the animal's physiology, though in subsequent tests a rigid head restraint was introduced to physically limit the maximum extension angle (Bostrom et al., 1996). Despite its advantages, this device was limited in its ability to precisely control head kinematic parameters. Servomotors were used in our device with the aim of programming and testing specific motion profiles with good accuracy and repeatability. As a result, parameters such as head retraction distance, extension angle, and speed/accelerations during whiplash motions can be systematically varied and their effects on the resulting pressure pulses and tissue injury can be independently studied.

Inert surrogate model

Prior to animal testing, an inert surrogate model was developed for the preliminary validation of the whiplash device. The surrogate model strictly functions to mimic the physical constraints of the biteplate and motor linkages during *in vivo* animal testing and does not attempt to produce a biofidelic response.

The surrogate model (Figure 2) consists of a 2'' diameter hose attached to a plate with an approximately 5 kg mass added to represent the animal's neck and head, respectively. The 5 kg mass was conservatively selected and represents approximately 25% of the body weight of the pigs that will eventually be tested with the device. The hose length was constrained to 30 cm from the plate using a U-bolt screwed to a wood board which was clamped to the operating table. The length of the hose approximates the neck length of the pig up to the T1 vertebra (Condotta et al.,

2018) as the animals will likely be constrained to the table via straps at this vertebral level similar to previous experiments (Svensson et al., 1993).

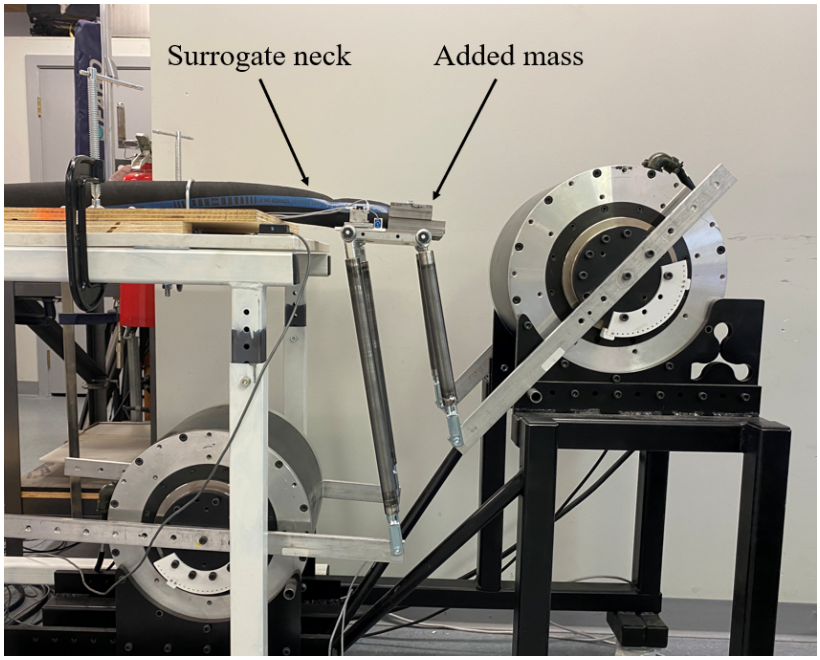

Figure 2: Surrogate model to represent the pig head and neck.

Tested motion profile

A motion profile was obtained through video marker tracking from previous (unpublished) porcine whiplash testing (Figure 3). These tests simulated whiplash motions using a mechanism similar to the device described in Svensson et al. (1993). This particular motion profile was selected as it models a relatively severe whiplash motion with a peak head extension angle of 80 degrees in approximately 70 ms. Previous human volunteer and post-mortem human subject (PMHS) testing of whiplash injury have involved sled tests with deltaV's up to 10 and 25 km/h, respectively (Szabo et al., 1994; Siegmund et al., 1997; Eichberger et al., 1998; Philippens et al., 2000; Kang et al., 2014) as most neck injuries from rear-end collisions were found to occur with deltaV's less than 20 km/h (Philippens et al., 2000). For comparison with our selected motion profile, rear-end PMHS testing around 20 km/h deltaV's produced maximum head extension angles of 50-60 degrees at around 200-250 ms (Bertholon et al., 2000; Philippens et al., 2000; Kang et al., 2014). Our selected motion profile represents an extreme upper end in terms of whiplash motion severity and is used here to discern the extent of the motor and device capabilities. If our device can reproduce this extreme motion, it will be capable of reproducing all other intermediate motion profiles.

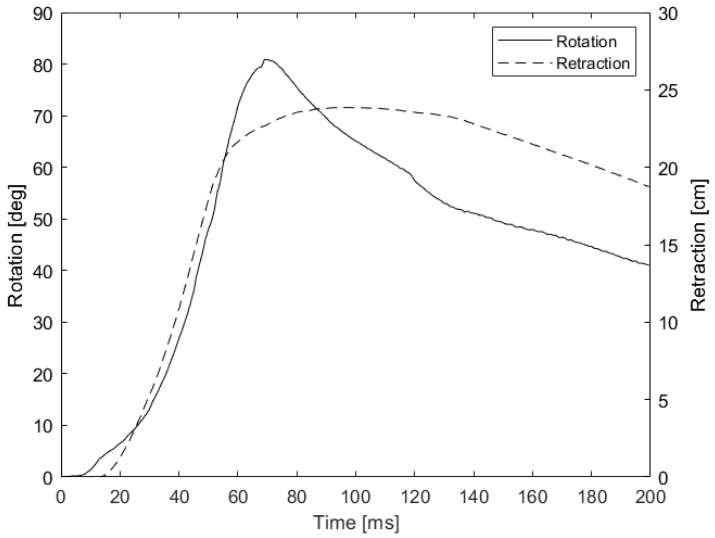

Figure 3: Original motion profile.

In order to incrementally test the device capabilities, the time scale of the selected motion profile was altered using a time factor (TF). Figure 4 shows the original motion profile (TF = 1) compared to the scaled motion profiles with TF = 8, 4, 3.5, 3, 2. A TF of 8 for example represents the same range of motion as the original profile over 8 times the time period.

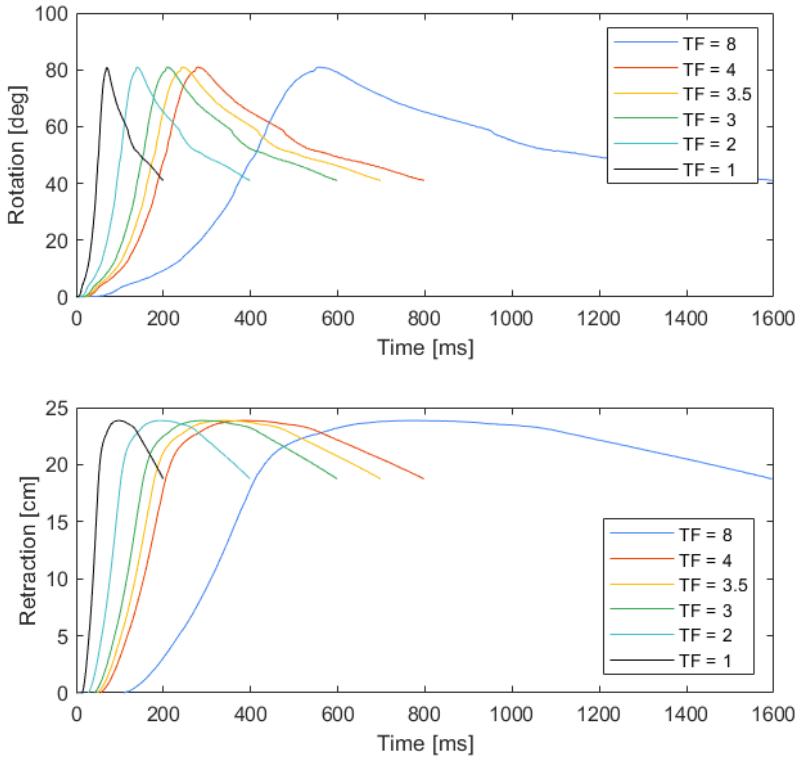

Figure 4: Scaled motion profiles.

A custom Matlab (R2019b, Mathworks Inc., Natick, MA) program was used to determine the required motor rotations to achieve the input motion profiles. The program output included incremental motor rotations which were then programmed and implemented using the NI-Motion module in Labview (2013SP1, National Instruments, Austin, TX). Motion profiles were incrementally tested starting with TF = 8 until an issue such as encoder following error or torque overload occurred. An intermediate motion profile (TF = 4) was tested three times to quantify the device repeatability.

Data collection and processing

The surrogate headplate was instrumented (Figure 5) with biaxial linear accelerometers (Endevco, 7265A, Irvine, CA) and a uniaxial angular rate sensor (DTS, ARS Pro, Seal Beach, CA). The controller voltage signal to the Motor 1 servo drive was also recorded in order to calculate the motor torque output. Motor 1 was selected for the torque calculations as it is the limiting motor due to its larger required range of motion. Data was recorded for 5 seconds at 10 kHz using a 16-bit DAQ card (PXI-6221, National Instruments, Austin, TX). All data channels conformed to SAE J211 Channel Class 1000 (SAE, 2003). Recorded instrumentation data was digitally low-pass filtered using Matlab according to Channel Class 1000.

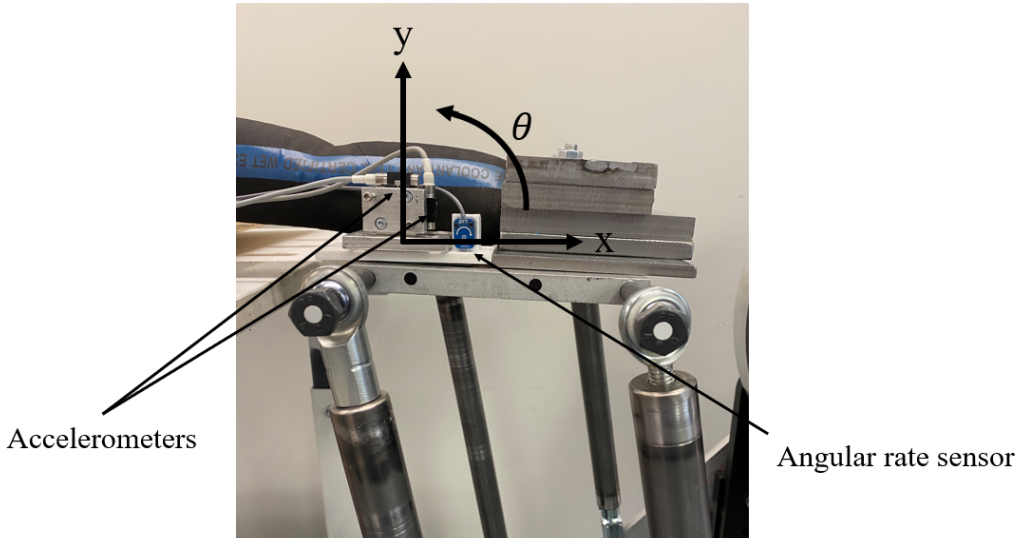

Figure 5: Instrumented plate.

Through Labview, the Motor 1 (M1) and Motor 2 (M2) encoder positions were logged at 100 Hz to capture the motor rotational positions. Positive motor rotation is counter clockwise for both motors from the view in Figure 2. Additionally, two markers were placed on the bolthead attaching the articulated arms to the headplate (white markers in Figure 5) and sagittal-view videos were captured at 240 fps using an iPhone 11 (Apple, Cupertino, CA). Markers were digitized using open-source software (Kinovea, https://www.kinovea.org/). Videos and instrumentation data were synchronized using an LED which turned on when the DAQ was triggered.

RESULTS

Incremental motion profiles

The plate rotation and retraction, M1 and M2 encoder positions, and M1 torque output are presented in Figure 6 (TF = 8 and 4), and 7 (TF = 3.5 and 3). The input values represent the programmed motion profiles while the output values represent the video marker tracking data (rotation and retraction), and the logged encoder positions (M1 and M2 position). Testing was completed up to TF = 3 as the M1 rated torque limit of 200 N·m was reached at this level at approximately 110 ms (Figure 7).

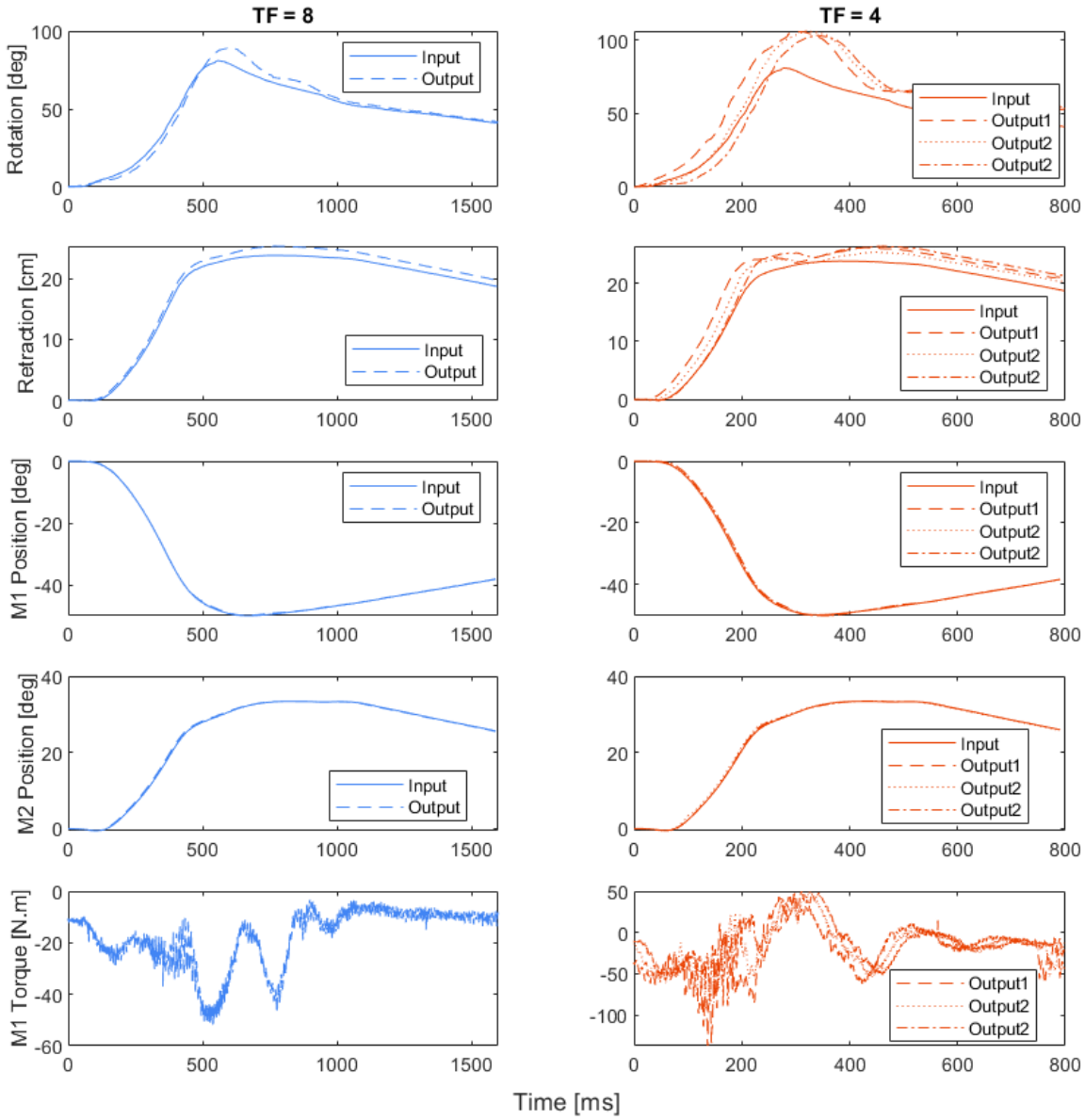

Figure 6: Position and torque data for TF = 8 and 4.

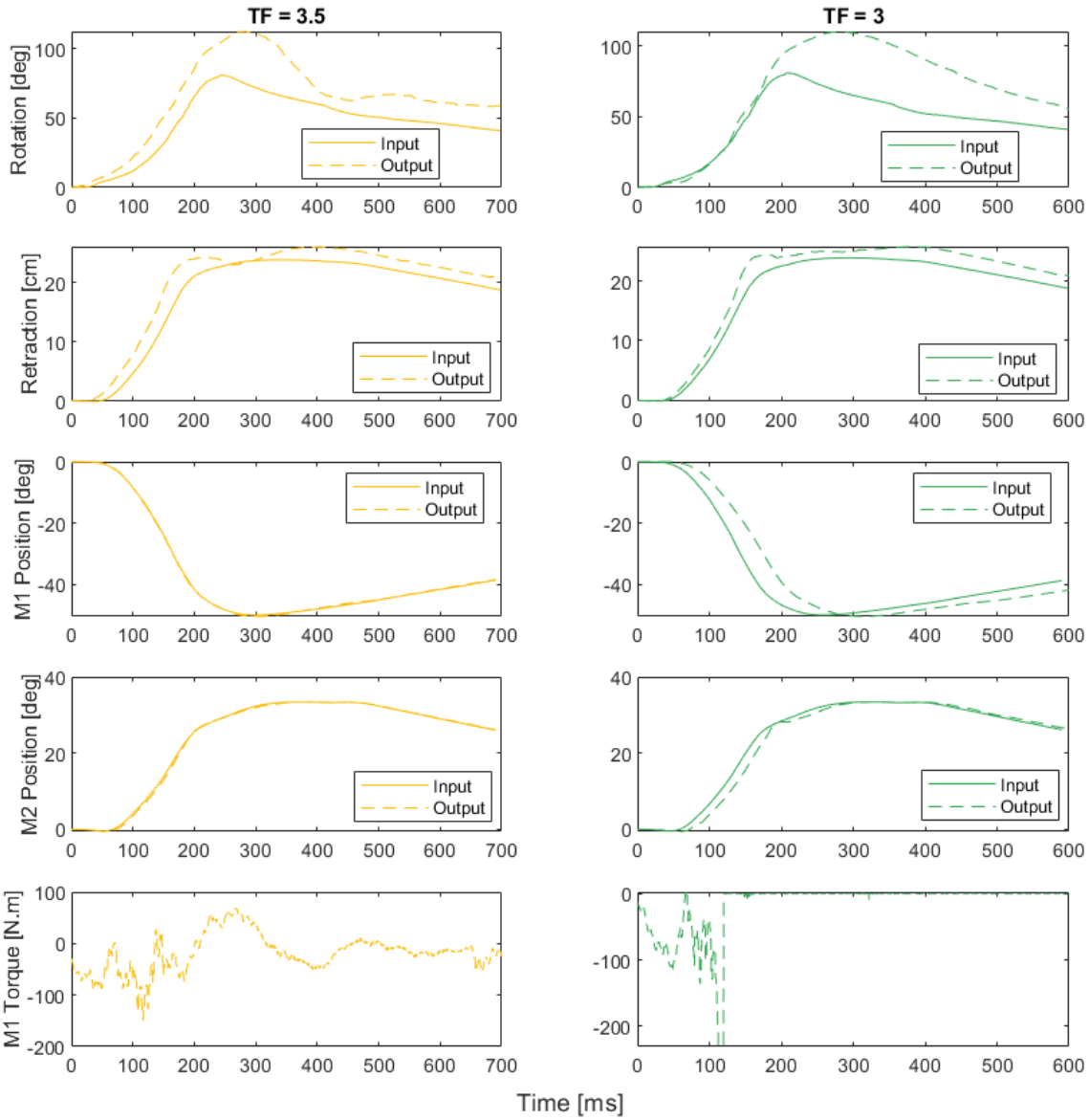

Figure 7: Position and torque data for TF = 3.5 and 3.

Figures 8 and 9 present the angular rate and acceleration data for TF = 8, 4, and TF = 3.5, 3, respectively. A peak angular rate, x acceleration and y acceleration of 16 rad/s, 9 g, and 3 g, were achieved with the TF = 3.5 motion profile, respectively. Prior to reaching the torque overload, the TF = 3 motion profile achieved a peak angular rate, x acceleration and y acceleration of 24 rad/s, 15 g, and 14 g, respectively

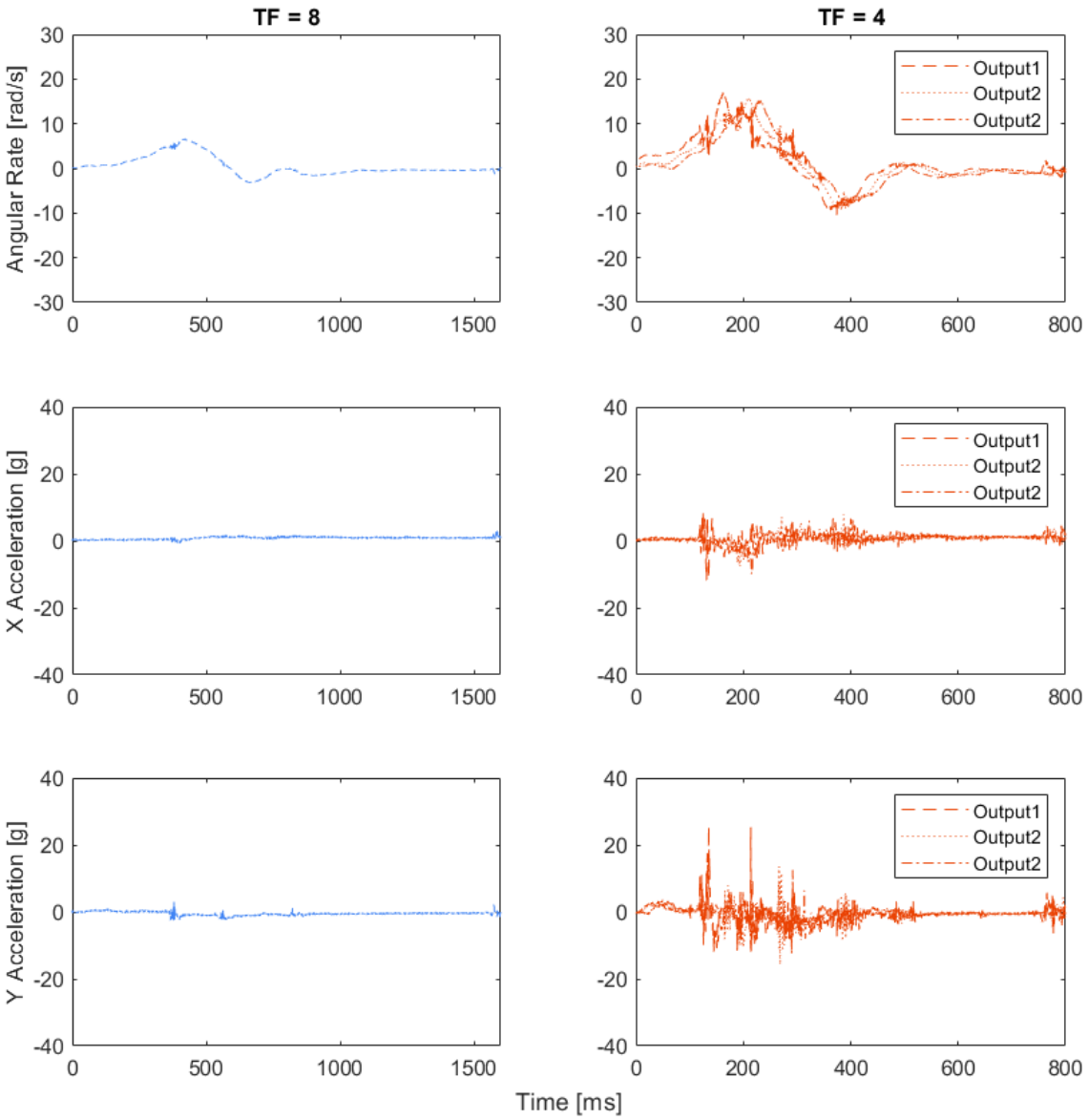

Figure 8: Angular rate and acceleration data for TF = 8 and 4.

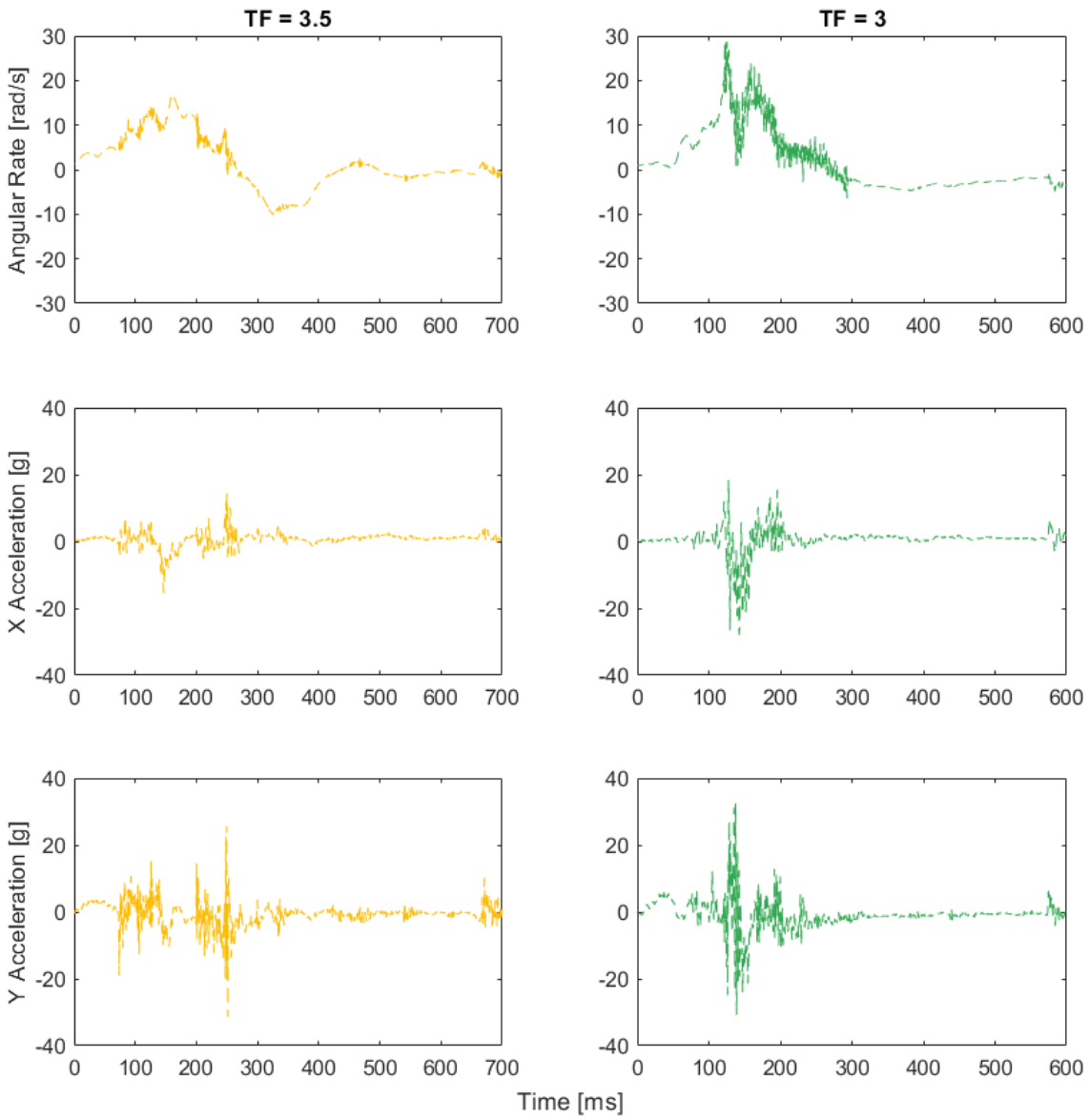

Figure 9: Angular rate and acceleration data for TF = 3.5 and 3.

Accuracy

From the data in Figures 6 and 7, the percent error between the input and output peak values and time-to-peak values were determined and are tabulated in Table 1. This data can be used to quantify the accuracy of the device in producing the programmed motion profiles. Time-to-peak and peak values for the rotation and retraction plots had percent errors up 39%. Percent errors for both motors were no more than 5% except for the TF = 3 case where the torque overload in M1 caused a delay in the time-to-peak.

Table 1: Percent error between input and output peak and time to peak values

	Rotation		Retraction		M1 Position		M2 Position	
TF	**Time-to-peak**	**Peak Value**	**Time-to-peak**	**Peak Value**	**Time-to-peak**	**Peak Value**	**Time-to-peak**	**Peak Value**
8	8%	10%	1%	6%	0%	0%	1%	0%
4	12%	31%	12%	10%	3%	1%	0%	0%
3.5	16%	39%	15%	9%	0%	1%	5%	0%
3	33%	36%	35%	8%	19%	1%	6%	0%

Repeatability

An intermediate motion profile (TF = 4) was tested three times to assess the repeatability of the produced motion profiles. Table 2 presents the mean, standard deviation (SD) and coefficient of variation (CoV) for the peak and time-to peak-values of the rotation, retraction, and M1 and M2 position traces. The time-to-peak and peak values for all traces had a CoV less than 5%.

Table 2: Mean, standard deviation and coefficient of variation between the TF = 4 trials (n = 3)

		Mean	SD	CoV
Rotation	**Time-to-Peak [ms]**	322	10	3%
	Peak value [deg]	105	2	2%
Retraction	**Time-to-Peak [ms]**	447	17	4%
	Peak value [cm]	26	1	2%
M1 Position	**Time-to-Peak [ms]**	350	0	0%
	Peak value [deg]	50	0	0%
M2 Position	**Time-to-Peak [ms]**	440	10	2%
	Peak value [deg]	33	0	0%

DISCUSSION

This project aimed to test and validate a new device which can simulate whiplash motions in a porcine model and attempts to address the limitations of previous designs. Our evaluation included assessing whether the device could replicate motion profiles from previous whiplash studies and to quantify the accuracy and repeatability of the simulated whiplash motions.

One relatively severe whiplash motion profile was selected from a previous porcine whiplash study to be replicated (Obj. 1). To assess the device and motor capabilities, the selected motion profile was scaled via a time factor and incrementally tested. With the current device design, we successfully replicated the selected motion profile when scaled with a TF = 3.5. This motion profile consisted of a peak extension angle of 80 degrees in approximately 250 ms which is representative of previous PMHS sled tests investigating cervical spine injuries from rear-end collisions (Bertholon et al., 2000; Philippens et al., 2000; Kang et al., 2014). With this motion profile, a peak angular rate of 16 rad/s and x and y accelerations of 15 and 30 g were achieved,

respectively. Peak resultant plate accelerations exceed the range of previous low-speed human volunteer rear-end collision studies (Siegmund et al., 1997) and are within range of the approximately 20 g head accelerations reached in previous porcine whiplash studies (Svensson et al., 1993).

A TF = 3 motion profile was also tested; however, M1 reached its rated torque limit within the first 110 ms where an initial rapid ramp up is required. This indicates a limitation of the current device design which prevents testing of higher severities. Several potential solutions can be implemented to address this limitation. Currently, the motor servo system is programmed to output a maximum current corresponding to the rated torque limit (200 N·m). However, the motors are capable of an instantaneous maximum torque up to 600 N·m. This maximum torque limit can be achieved for intermittent periods which is adequate for the short period in our whiplash motion profiles. To harness the maximum torque limit, the motor servo system can be reprogrammed. Another potential solution can be to optimize the lengths of the linkages attached to the motors to reduce the torque load on M1 at the initial ramp up period of the motion profile. Additionally, with the current setup, most of the added mass on the plate is biased towards M1. Redistributing the mass to better represent the position of the porcine head center of gravity may help offload M1 and improve the device's ability to generate the extreme pulse selected. These potential solutions will be explored in future work.

Several measurements were made to assess how accurately programmed motion profiles could be replicated with our device (Obj. 2). Marker tracking from digitized videos were used to assess the rotation and retraction of the headplate while logged encoder positions were used to assess the angular positions of the motors. Accuracy and repeatability assessments were conducted using the magnitude of the peak values and time-to-peak points of the motion profile traces as these quantities represent the fundamental characteristics of the motion profiles. The plate rotation and retraction had percent errors up to 39% which increased with decreasing TF. Additionally, in all cases for rotation, the peak value percent error was larger than the time-to-peak percent error. These large percent errors for the plate rotation and retraction can be attributed to several factors. First, the behavior of the plate is largely dependent on the behavior of the hose used as the surrogate neck. From the recorded videos, we visually observed that at the lower TF cases, the hose exhibited buckling near the plate attachment point which resulted in larger rotation angles. This limitation will be addressed in subsequent work where the surrogate head and neck model will be replaced with cadaver pigs which will elicit a more biofidelic response. Additionally, some discrepancy in the plate rotation and retraction measurements can be attributed to lens distortion error which was not corrected for as well as errors in spatial calibration and marker tracking. However, as expected, at the motor level, motor angular positions had percent errors no more than 5% for tests with TF = 3.5 and larger.

An intermediate motion profile (TF = 4) was tested three times to assess the repeatability of the produced motion profiles (Obj. 2). Despite the overshoot of the plate rotation and retraction from the buckling of the hose which affected accuracy, motion profiles were produced with good repeatability. Coefficient of variation values were below 5% for all measured quantities. The good repeatability of this proposed device is a significant strength compared to previous designs.

This new proposed device aims to simulate whiplash motions in a porcine model and address the limitations of previous work. Our preliminary assessment of this device indicates that it has potential to enable further study of the DRG whiplash injury mechanism by producing specific programmed motion profiles with good accuracy and repeatability. With some additional improvements, this device can be used in future studies to systematically investigate the effect of various head and neck kinematic parameters on the measured spinal pressures during simulated whiplash. Subsequent validation and testing of this device will involve design changes to achieve the whiplash severities tested in previous studies. Additionally, the device will be further validated using cadaver porcine testing prior to *in vivo* experiments.

CONCLUSIONS

Preliminary assessment of a new whiplash simulation device indicates promising potential for it to address specific limitations of previous methods used to study whiplash injury in a porcine model. The current device enables more accurate and repeatable control of specific programmed motion profiles. This capability can be used in future porcine studies to further elucidate the DRG whiplash injury mechanism by correlating head and neck kinematics parameter to measured spinal pressures and tissue damage. Through subsequent design modifications, the device's capabilities will be optimized to reach the severe whiplash motion severities tested in previous porcine whiplash studies. Improving our understanding of the whiplash injury mechanism is an important step to treating and ultimately preventing this poorly understood affliction.

ACKNOWLEDGEMENTS

Thank you to Jeff Nickel and Mircea Oala-Florescu of MEA Forensic Engineers & Scientists for their technical support and contributions to the whiplash device development. The authors also acknowledge funding support from the Natural Sciences and Engineering Research Council of Canada and the Insurance Institute for Highway Safety.

REFERENCES

ALDMAN, B. (1986). An analytical approach to the impact biomechanics of head and neck injury, 30th Annual Proceedings American Association for Automotive Medicine, pp. 439–454.

BERTHOLON, N., ROBIN, S., LE-COZ, J., POTEIR, P., LASSAU, J. AND SKALLI, W. (2000). Human head and cervical spine behaviour during low-speed rear-end impacts: PMHS tests with a rigid seat, IRCOBI Conference.

BOSTROM, O. ET AL. (1996). A New Neck Injury Criterion Candidate Based on Injury Findings in the Cervical Spine Ganglia after Experimental Sagittal Whiplash, Ircobi, pp. 123(119)-136(133).

BUSSCHER, I., PLOEGMAKERS, J. J. W., VERKERKE, G. J. AND VELDHUIZEN, A. G. (2010). Comparative anatomical dimensions of the complete human and porcine spine, European Spine Journal, 19(7), pp. 1104–1114. doi: 10.1007/s00586-010-1326-9.

CONDOTTA, I., BROWN-BRANDL, T., STINN, J. AND DAVIS, J. D. (2018). Dimensions of the Modern Pig, American Society of Agricultural and Biological Engineers, (February 2019). doi: 10.13031/trans.12826.

CROFT, A. C., HERRING, P., FREEMAN, M. D. AND HANELINE, M. T. (2002). The neck injury criterion: Future considerations, Accident Analysis and Prevention, 34(2), pp. 247–255. doi: 10.1016/S0001-4575(01)00020-3.

CURATOLO, M., BOGDUK, N., IVANCIC, P. C., MCLEAN, S. A., SIEGMUND, G. P. AND WINKELSTEIN, B. A. (2011). The role of tissue damage in whiplash-associated disorders, Spine, 36(25), pp. S309–S315. doi: 10.1097/BRS.0b013e318238842a.

DUHAIME, A. C. (2006). Large animal models of traumatic injury to the immature brain, Developmental Neuroscience, 28(4–5), pp. 380–387. doi: 10.1159/000094164.

EICHBERGER, A., STEFFAN, H., GEIGLE, B., SVENSSON, M. Y., BOSTRÖM, O., LEINZINGER, P. E. AND DAROK, M. (1998). Evaluation of the applicability of the neck injury criterion in rear end impacts on the basis of human subject tests, IRCOBI Conference, pp. 321–333. doi: 10.1016/B978-0-323-07980-8.00006-0.

EICHBERGER, A., DAROK, M., STEFFAN, H., LEINZINGER, P. E., BOSTRÖM, O. AND SVENSSON, M. Y. (2000). Pressure measurements in the spinal canal of post-mortem human subjects during rear-end impact and correlation of results to the neck injury criterion, Accident Analysis and Prevention, 32(2), pp. 251–260. doi: 10.1016/S0001-4575(99)00097-4.

JONES, C. F., LEE, J. H. T., KWON, B. K. AND CRIPTON, P. A. (2012). Development of a large-animal model to measure dynamic cerebrospinal fluid pressure during spinal cord injury: Laboratory investigation, Journal of Neurosurgery: Spine, 16(6), pp. 624–635. doi:

10.3171/2012.3.SPINE11970.

KANG, Y. S., MOORHOUSE, K., ICKE, K., HERRIOTT, R. AND BOLTE, J. (2014). Head and cervical spine responses of post mortem human subjects in moderate speed rear impacts, IRCOBI Conference, pp. 268–285.

LEE, J. H. T. *ET AL.* (2013). A Novel porcine model of traumatic thoracic spinal cord injury, Journal of Neurotrauma, 30(3), pp. 142–159. doi: 10.1089/neu.2012.2386.

ONO, K. AND KANNO, M. (1993). Influences of the physical parameters on the risk to neck injuries in low impact speed rear-end collisions, Accident Analysis and Prevention, 28(4), pp. 493–499. doi: 10.1016/0001-4575(96)00019-X.

ÖRTENGREN, T., HANSSON, H. A., LÖVSUND, P., SVENSSON, M. Y., SUNESON, A. AND SALJÖ, A. (1996). Membrane leakage in spinal ganglion nerve cells induced by experimental whiplash extension motion: A study in pigs, Journal of Neurotrauma, 13(3), pp. 171–180. doi: 10.1089/neu.1996.13.171.

PHILIPPENS, M., WISMANS, J., CAPPO, H., YOGANANDAN, N. AND PINTAR, F. (2000). Whole body kinematics using post mortem human subjects in experimental rear impact, IRCOBI Conference, (4), pp. 363–378.

SAE. (2003). *Instrumentation for Impact Test-Part1-Electronic Instrumentation (SAE J211-1 Dec 03)*, SAE International.

SHENG, S. R., WANG, X. Y., XU, H. Z., ZHU, G. Q. AND ZHOU, Y. F. (2010). Anatomy of large animal spines and its comparison to the human spine: A systematic review, European Spine Journal, 19(1), pp. 46–56. doi: 10.1007/s00586-009-1192-5.

SHENG, S. R., XU, H. Z., WANG, Y. L., ZHU, Q. A., MAO, F. M., LIN, Y. AND WANG, X. Y. (2016). Comparison of cervical spine anatomy in calves, pigs and humans, PLoS ONE, 11(2), pp. 1–10. doi: 10.1371/journal.pone.0148610.

SIEGMUND, G. P., KING, D. J., LAWRENCE, J. M., WHEELER, J. B., BRAULT, J. R. AND SMITH, T. A. (1997). Head / Neck Kinematic Response of Human Subjects in Low-Speed Rear-End Collisions, Society of Automotive Engineers.

SIEGMUND, G. P., WINKELSTEIN, B. A., IVANCIC, P. C., SVENSSON, M. Y. AND VASAVADA, A. (2009). The Anatomy and biomechanics of acute and chronic whiplash injury, Traffic Injury Prevention, 10(2), pp. 101–112. doi: 10.1080/15389580802593269.

STERNER, Y. AND GERDLE, B. (2004). Acute and chronic whiplash disorders - A review, Journal of Rehabilitation Medicine, 36(5), pp. 193–210. doi: 10.1080/16501970410030742.

SVENSSON, M. Y., ALDMAN, B., HANSSON, H. A, LÖVSUND, P., SEEMAN, T.,

SUNESON, A. AND ÖRTENGREN, T. (1993). Pressure Effects in the Spinal Canal during Whiplash Extension Motion: A Possible Cause of Injury to the Cervical Spinal Ganglia, IRCOBI Conference, pp. 189–200.

SVENSSON, M. Y., BOSTRÖM, O., DAVIDSSON, J., HANSSON, H. A., HÅLAND, Y., LÖVSUND, P., SUNESON, A. AND SÄLJÖ, A. (2000). Neck injuries in car collisions - A review covering a possible injury mechanism and the development of a new rear-impact dummy, Accident Analysis and Prevention, 32(2), pp. 167–175. doi: 10.1016/S0001-4575(99)00080-9.

SZABO, T. J., WELCHER, J. B., ANDERSON, R. D., RICE, M. M., WARD, J. A., PAULO, L. R. AND CARPENTER, N. J. (1994). Human occupant kinematic response to low speed rear-end impacts, SAE Technical Papers, 103, pp. 630–642. doi: 10.4271/940532.

YAO, H. D., SVENSSON, M. Y. AND NILSSON, H. (2016). Transient pressure changes in the vertebral canal during whiplash motion - A hydrodynamic modeling approach, Journal of Biomechanics, 49(3), pp. 416–422. doi: 10.1016/j.jbiomech.2016.01.005.